

# A novel biodegradable ESERS (enhanced SERS) platform with deposition of Au, Ag and Au/Ag nanoparticles on gold coated zein nanophotonic structures for the detection of food analytes

Xiaoyuan Ma<sup>a,b</sup>, Hazal Turasan<sup>a</sup>, Fei Jia<sup>c</sup>, Sujin Seo<sup>d</sup>, Zhouping Wang<sup>b</sup>, Gang Logan Liu<sup>d</sup>, Jozef L. Kokini<sup>a,\*</sup>

<sup>a</sup> Department of Food Science, Purdue University, West Lafayette, Indiana, USA

<sup>b</sup> School of Food Science and Technology, Jiangnan University, Wuxi, China

<sup>c</sup> College of Food Science, China Agricultural University, Beijing, China

<sup>d</sup> Electrical & Computer Engineering, University of Illinois at Urbana-Champaign, Illinois, USA

## ARTICLE INFO

### Keywords:

SERS platform  
Gold coated zein  
Biodegradable  
Nanoparticle decoration  
Nanophotonic structures

## ABSTRACT

In this paper we studied the fabrication of a family of new biodegradable SERS sensors using a gold coated zein film with inverted pyramid structures that we had fabricated previously and coupled it with deposition of gold, silver and silver-shelled-gold nanoparticles. The proximity and contact between the gold surface and the new added nanoparticles help create new hot spots, which enhance the SERS intensity. Rhodamine 6 G was used as the Raman active molecule to evaluate the SERS enhancement effect. Results revealed that different nanoparticles exhibit different SERS effects. Silver-shelled-gold nanoparticles gave the highest enhancement factor of  $3 \times 10^5$  followed by silver and gold nanoparticles relative to a glass surface. The enhancement factor of the new silver-shelled-gold nanoparticle decorated platform with the best performance relative to the gold coated zein nanophotonic structures is  $10^2$ , a remarkable improvement. This sensitivity improvement takes the newly developed zein based biodegradable SERS biosensor platform one step closer to non-biodegradable sensors.

## 1. Introduction

Since Fleischman first used the roughened silver electrode to obtain the Raman spectra of pyridine molecules in 1974 [1], SERS has been widely used in mapping technology and single molecule detection [2–6]. The traditional SERS substrates include: roughened metal electrodes, metal nanoparticles, roughened metal films, etc. In recent years, the three-dimensional nanostructure complexes including bimetallic nanoparticles such as gold coated silver nanoparticles or hollow nanoparticles have emerged and widespread attention has been given to them due to their unique optical characteristics which contribute to the enhancement of the Raman signal [7–9].

SERS is an excellent method for the detection of toxic and allergic food contaminants, due to its ability to detect very low concentrations of analytes, even single molecules [10]. For example, with SERS, restricted antibiotics were detected with a limit of detection of 20 ppb [11], real-time monitoring of pesticides can be conducted directly on plant tissues [12,13]. In-situ SERS detection of three gram-positive

bacteria, *Staphylococcus xylosum*, *Listeria monocytogenes*, and *Enterococcus faecium* was successfully conducted with limits of detections of 50, 100, and 100 CFU/mL, respectively [14]. Food adulterants, such as melamine, have been detected with very low limits of detection using SERS [15]. Pharmaceutical compounds can also be detected with limit of detection levels reaching ng/ml using nanostructured SERS platforms [16].

Despite these successful measurements, the use of synthetic polymers and plastics for the fabrication of SERS platforms is gradually becoming an issue from the sustainability point of view, as the used/disposed sensor platforms take many years to fully degrade in the environment. For this reason, in our group we are focusing on fabricating environmentally friendly, biodegradable green alternatives to the plastic-based biosensors [17–19]. Our team has developed an innovative biodegradable protein-based SERS sensor platform using corn zein with replicating nanophotonic structures using soft lithography [17,18,20–22]. Briefly, the nanophotonic structures were first transferred to polydimethylsiloxane (PDMS) films from a PET master molds

\* Corresponding author.

E-mail addresses: [mxy@jiangnan.edu.cn](mailto:mxy@jiangnan.edu.cn) (X. Ma), [hturasan@purdue.edu](mailto:hturasan@purdue.edu) (H. Turasan), [jiafei@cau.edu.cn](mailto:jiafei@cau.edu.cn) (F. Jia), [seo46@illinois.edu](mailto:seo46@illinois.edu) (S. Seo), [wangzp@jiangnan.edu.cn](mailto:wangzp@jiangnan.edu.cn) (Z. Wang), [loganliu@illinois.edu](mailto:loganliu@illinois.edu) (G.L. Liu), [jkokini@purdue.edu](mailto:jkokini@purdue.edu) (J.L. Kokini).

<https://doi.org/10.1016/j.vibspec.2019.103013>

Received 7 August 2019; Received in revised form 10 November 2019; Accepted 16 December 2019

Available online 17 December 2019

0924-2031/ © 2019 Published by Elsevier B.V.

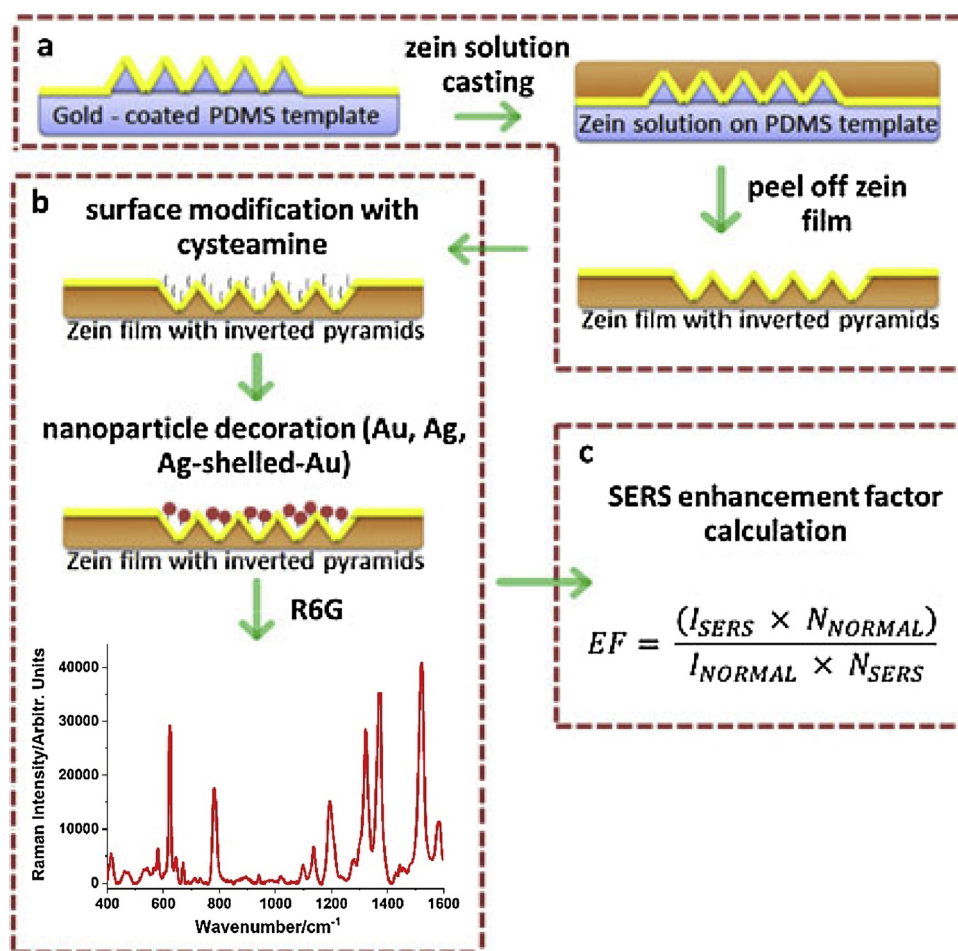


Fig. 1. The diagram for fabrication of zein film sensor and its detection of R6G.

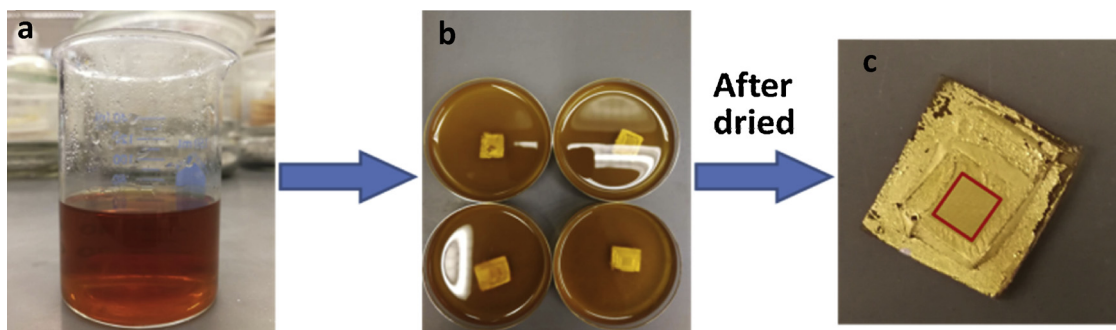


Fig. 2. Photographs of the zein film preparation; a) zein solution before casting, b) zein solutions cast on gold coated PDMS films, c) peeled off zein films from PDMS layers with complete gold layer transfer. Red square shows the nanophotonic region on zein film surface.

and coated with gold. Zein solutions were then cured on top of the gold coated PDMS films and peeled off, with excellent and unanticipated fidelity leading to a complete transfer of nanostructures and the gold layers. Out of inverted nanopyramid, nanopore and nanodome structures, inverted nanopyramids gave the highest enhancement factor of  $10^4$  relative to a flat glass surface. These zein based SERS sensors were then successfully used in the detection of acrylamide, a food toxin, and Ara h1 the main peanut allergen protein [20,21]. In our recent study, we were able to increase the SERS enhancement factor of zein-based SERS platforms twice, with the decoration of gold nanoparticles on the surface of gold coated nanostructured zein platforms [18]. This enhancement enabled detection of pyocyanin, the lethal toxin of water-borne pathogen *Pseudomonas aeruginosa*, from water with a detection level of

25  $\mu\text{M}$ . Even though SERS enhancement factor of zein-based platforms was increased with the decoration of Au nanoparticles, there is still room for improving the sensitivity to match the sensitivity of plastic-based SERS platforms.

Another recent study confirms that SERS enhancement increases significantly when gold coated nanocup array SERS substrates were additionally decorated with metallic nanoparticles [23]. Decoration of a gold layer coated flat surface with Au nanoparticles increased SERS signal 6 times relative to the gold layer coated flat surface while Au nanoparticle decoration onto a gold coated nanocup array instead of gold coated flat surface increased the SERS signal 25 times. This study shows, a more sensitive SERS biosensor platform can be achieved, due to a higher number of hotspot formation, by incorporating

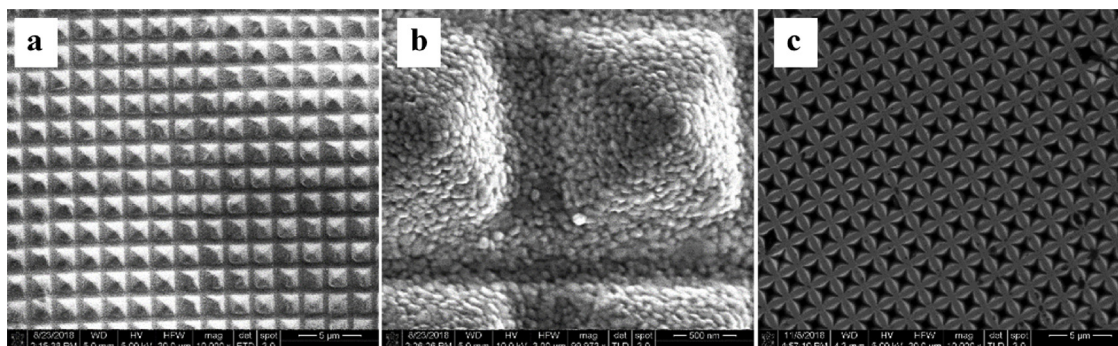


Fig. 3. SEM images of PDMS based films with positive pyramid structures (a and b) and zein based films with inverted pyramid structures (c).

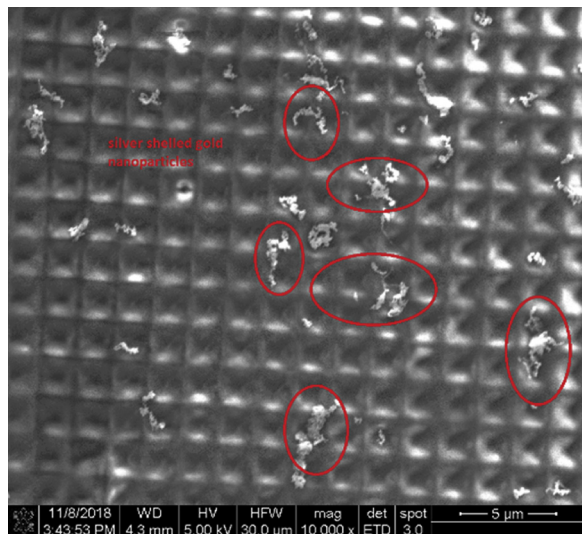


Fig. 4. SEM images of silver-shelled-gold nanoparticles decorated on the surface of gold coated zein films with inverted pyramid structures.

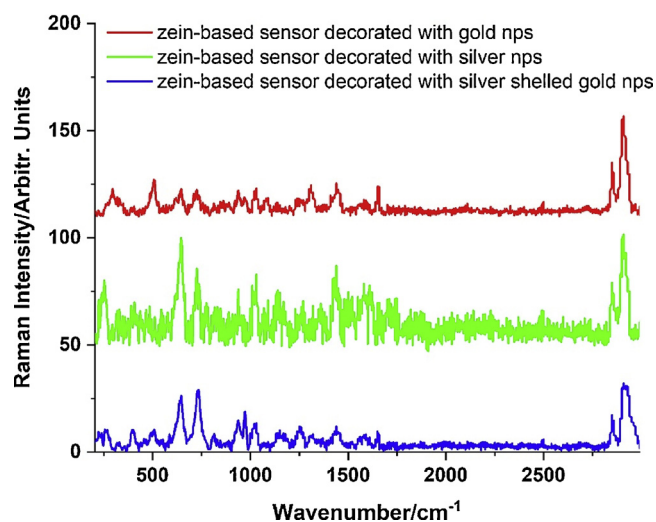


Fig. 5. Raman spectra of 200 nm gold layer coated nanostructured zein-based sensors decorated with gold (red), silver (green), and silver shelled gold (blue) nanoparticles using cysteamine as the linker molecule.

nanoparticles on the surface of nanostructured arrays.

The use of bimetallic nanostructures for SERS detections have been shown to have advantages over monometallic structures. Bimetallic nano-mushroom structures were created by orienting the growth of silver on the surface of DNA-modified gold nanoparticles, and the

enhancement factor of  $10^9$  was achieved [24]. When bimetallic core-shell nanoparticles of gold and silver were compared to monometallic gold or silver nanoparticles, the SERS enhancement factor was found to be the highest for gold core-silver shell nanoparticles [25]. Gold/silver core-shell nanorods were compared with gold nanorods for the SERS detection of human immunoglobulin G with a detection limit of 70 fM was achieved with gold/silver core-shell nanorods, which was  $10^4$  times lower than the limit of detection of gold nanorods [26].

The goal of the study is to further increase the sensitivity of nanostructured zein-based SERS platforms by decorating the surface with gold, silver and bimetallic silver-shelled-gold nanoparticles. The effects of surface decoration with silver, gold and silver-shelled-gold nanoparticles separately on the enhancement of the SERS intensity was investigated using Rhodamine 6 G as the Raman active molecule. In addition, the enhancement created by the same concentration of nanoparticles deposited on a glass surface was also studied to offer a comparison between the SERS performance of a non-biodegradable surface with a biodegradable sensor platform.

## 2. Materials and methods

### 2.1. Materials

Ethyl Alcohol (140 Proof) was purchased from Decon Laboratories Inc. (King of Prussia, PA); Zein (Z3625), cysteamine (98 %), glutaraldehyde (GDA) (25 % in water solution) and Rhodamine-6 G (R6 G) were obtained from Sigma-Aldrich (St. Louis, MO); Oleic Acid (OA) (technical grade 90 %) from Alfa Aesar (Ward Hill, MA); mono-diglyceride emulsifier (BFP 65 K 1004200364) from Caravan Ingredients (Lenexa, KS); Acrylamide (98.5 %) was purchased from Fisher Scientific (Pittsburgh, PA). Au and Ag nanoparticles with 20 nm diameters were purchased from Ted Pella Inc. (Redding, CA) at  $7.0 \times 10^{11}$  and  $7 \times 10^{10}$  particles/ml concentrations, respectively. Silver shelled gold nanoparticles with a total diameter of 20 nm and a shell thickness of 6.4 nm were purchased from nanoComposix (San Diego, CA) at a concentration of  $2.6 \times 10^{13}$  particles/ml. To show the suspension stability of the nanoparticles, zeta potentials of the nanoparticles in deionized water were measured. The average zeta potentials were -30.0 mV, -47.17 mV, and -31.03 mV for silver-shelled-gold, silver and gold nanoparticles, respectively. These zeta potentials which are larger than -30 mV show that all nanoparticles repulse one another and the nanosized organization of the nanoparticles remains stable.

### 2.2. Preparation of zein films with inverted pyramid structures

Zein solutions were prepared following our methodology reported before [27]. Briefly, the zein protein was dissolved in 70 % ethanol at a 1:5 w/v ratio and heated to 62 °C and oleic acid (OA) plasticizer and mono/diglyceride emulsifier were added. Then glutaraldehyde was added for crosslinking in the ratio of 4 % glutaraldehyde to zein (w/w)

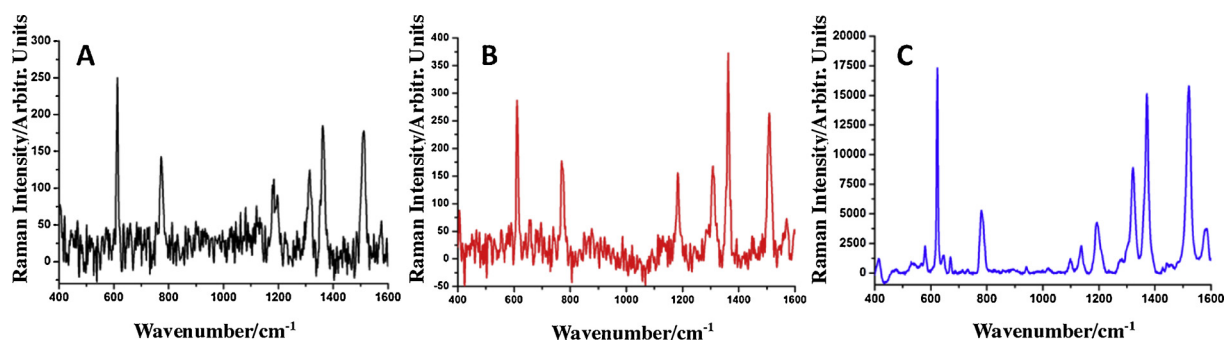


Fig. 6. (A) Raman spectra of 10 mM R6 G on a glass slide (B) SERS spectra of 10 mM R6 G on zein film with only inverted pyramid structures but no layer of gold (C) SERS spectra of 10 mM R6 G on zein film with both inverted pyramid structures and a 200 nm layer of gold.

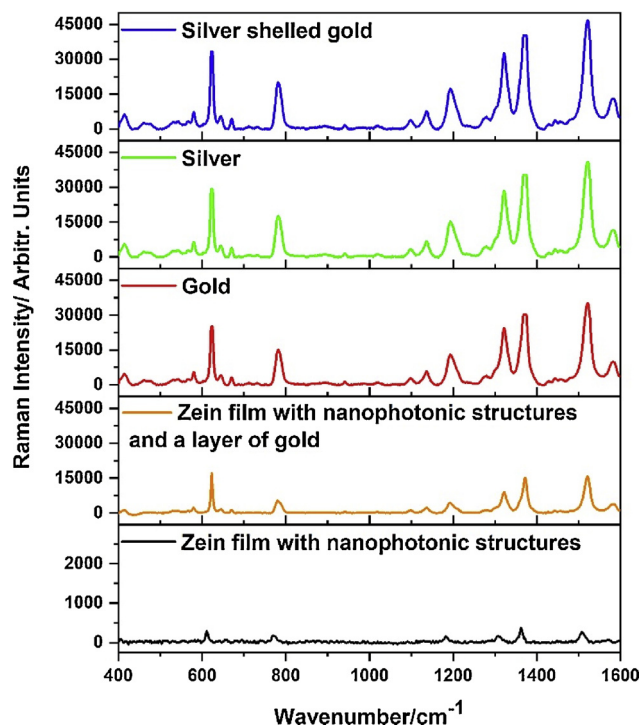


Fig. 7. SERS measurement of 0.1 mM R6 G using different nanoparticles decorated zein film sensor compared with zein film with inverted pyramid structures and a 200 nm layer of gold using 10 mM of R6 G (orange) and with the zein film with inverted pyramid structures (black).

stirred for 1 h, after heating to cool the solution to room temperature.

For the preparation of zein films with inverted pyramid structures, the gold coated PDMS films with positive pyramids with dimensions of  $2 \times 2 \times 2.1 \mu\text{m}$  were obtained from Dr. Logan Liu's laboratory at the University of Illinois and used as template [17,20]. Other aspects of this fabrication procedure were also discussed before. The zein solution mixture was then poured onto petri dishes with a 60 mm diameter with the PDMS template already in it. Then, zein films were peeled off from the PDMS template and complete transfer of nanostructures covered with gold onto zein was achieved. The final product consisted of zein films fabricated with inverted pyramid structures.

### 2.3. Decoration of different nanoparticles on the surface of zein films

The SERS effect of the deposition of different nanoparticles (gold, silver and silver-shelled-gold nanoparticles) chemically bound onto the surface of zein films with inverted pyramid structures was investigated. Cysteamine was used to fix the nanoparticles on the gold surface of zein films through its thiol group and an amine group at each end forming

an Au-S bond. The amine group is positively charged while the three (Au, Ag and Au/Ag) nanoparticles are all negatively charged with the use of a citrate-capping layer and the amine group electrostatically attracts the nanoparticles [27]. First, a 25  $\mu\text{L}$  droplet of 100 mM cysteamine was placed on the surface of the gold coated zein films. The film was then left at room temperature for 2 h to allow cysteamine to bind to the gold layer. The film was then washed using milli-Q water to remove the excess unbonded and free cysteamine and dried with a stream of nitrogen gas for a firm linkage. Five consecutive drops of 20 nm gold nanoparticles solution (10  $\mu\text{L}/\text{drop}$ ,  $7 \times 10^{10}$  particles/mL) were then placed on the zein film to fabricate the gold coated nanoparticle added zein sensor. The sensor was placed in a petri dish, covered and placed in the refrigerator at a temperature of 4  $^{\circ}\text{C}$  for 24 h [27] to enable bonding of gold nanoparticles to cysteamine. The zein sensors were then washed with milli-Q water and dried with nitrogen gas so that only the bonded nanoparticles remain on the sensor surface. The zein sensors decorated with 20 nm silver nanoparticles and 20 nm silver-shelled-gold nanoparticles followed the same procedure as gold nanoparticles.

### 2.4. SERS Detection of Rhodamine 6 g

For the deposition of Rhodamine 6 G (R6 G) molecules on various platforms tested in this study, the drop deposition technique was used, following our previously developed method [17,19,28]. To show the good distribution obtained with drop deposition technique, Raman spectra of R6 G molecules were taken from multiple spots on a flat glass surface. The replications, given in Supplemental Fig. 1, show that drop deposition technique is a technique that gives reproducible results when measurements are conducted at many points along the dried R6 G molecules.

First, Raman spectra of 10 mM Rhodamine 6 G (R6 G) was obtained directly on the glass slide, zein film with only nanophotonic structures and no gold, and zein film with nanophotonic structures and a 200 nm layer of gold, following our previously developed method [17]. Then, in order to compare the effect of the deposition of nanoparticles on enhancement of SERS intensity, 0.1 mM R6 G was placed on the surface of nanoparticle decorated zein sensors. Their SERS spectra with R6 G were obtained and used for SERS enhancement factor calculation.

Raman and SERS spectra were collected using a Thermo Scientific DXR2 Raman Microscope. The laser used had a wavelength of 633 nm and a power of 2 mW. An objective lens with 50x magnification was used in Raman microscope. A 25  $\mu\text{m}$  pinhole aperture was used to collect Raman scattering, which gave a total laser spot size of 1.3  $\mu\text{m}$ . The Raman measurements were repeated 3 times and the averages were obtained using the OMNIC software.

### 2.5. Scanning Electron microscopy

Scanning electron microscopy images of the samples were taken

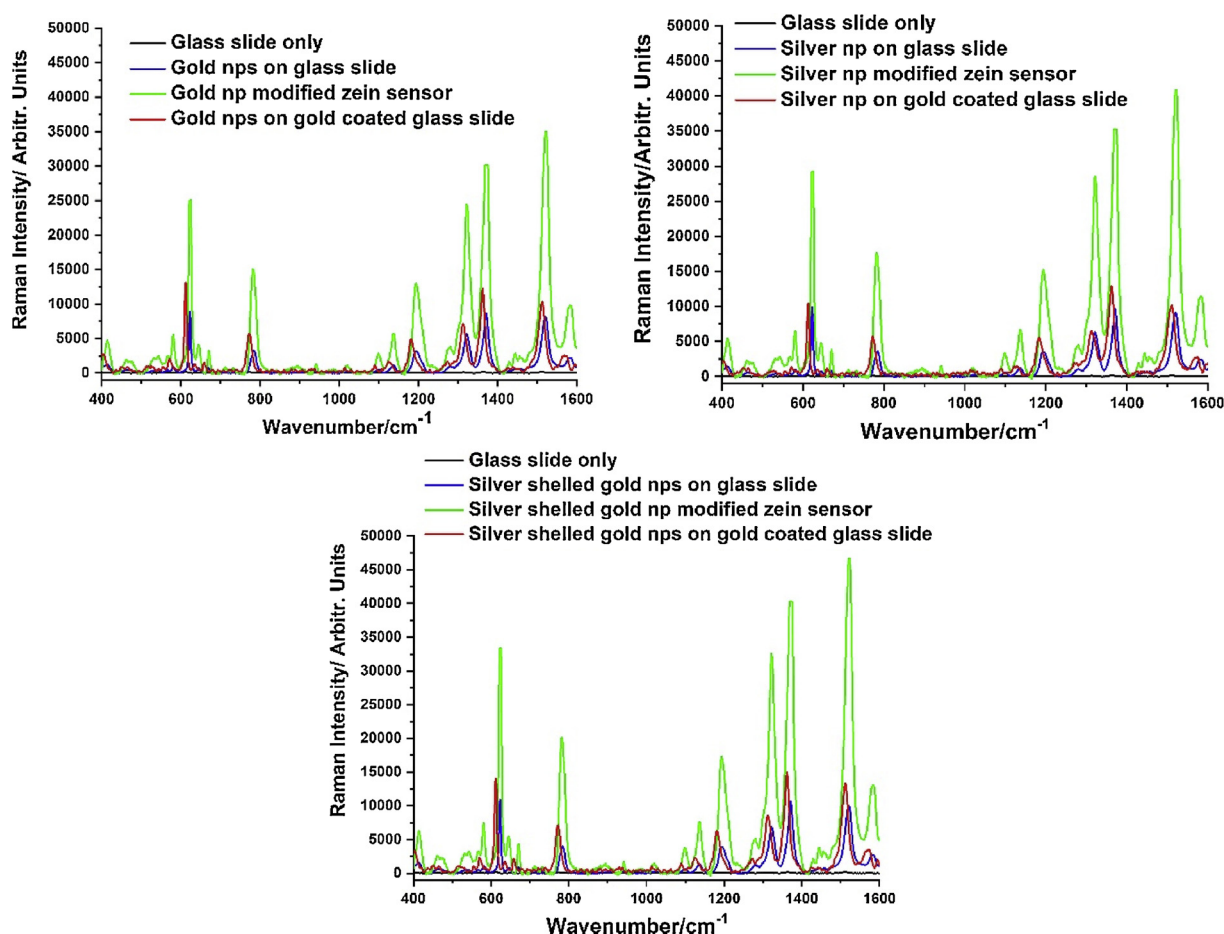


Fig. 8. SERS intensity of Rhodamine 6 G measured with nanoparticle decorated zein film sensors, nanoparticle decorated gold coated glass slides, nanoparticle decorated glass slides, and directly on glass slide.

with a Nova NanoSEM 200, using ETD and TLD detectors to visualize the deposition of nanoparticles on the gold coated surface. 1 cm x 1 cm pieces were cut from samples and fixed on SEM discs with double sided tape. During imaging, working distance was kept in the range of 4.3 mm–5.0 mm, with an accelerating voltage range of 5.00 kV–10.00 kV and a spot size of 3.0 nm. No additional metal coating was applied to the samples, since all the imaged samples were already coated with a 200 nm thick gold layer.

### 3. Results and discussion

#### 3.1. Preparation of gold coated inverted pyramid zein films and their decoration with gold, silver and silver-shelled-gold nanoparticles

The fabrication process of the nanoparticle decorated nanostructured zein film sensor platforms and the detection of R6 G using this platform is schematically illustrated in Fig. 1. The fabrication of gold coated nanostructured zein films follows our earlier studies [17], where gold coated PDMS films with positive pyramid structures were used as the template to transfer the nanopyramid structures and the gold layer onto the zein film surface using soft lithography (Fig. 1a). After the 200 nm gold layer and the nanopyramid structures were transferred to cast zein films, as a new strategy 20 nm nanoparticles of gold, silver and silver-shelled-gold were used to decorate the surface of nanostructured zein films using cysteamine as a binding agent (Fig. 1b). The SERS enhancement as a result of the addition of different nanoparticles using R6 G spectra were then used for SERS enhancement factor calculations (Fig. 1c).

#### 3.2. Characterization of the zein based SERS platforms with SEM imaging

The effectiveness of gold coated nanophotonic zein film preparation can be clearly seen in Fig. 2c, where the peeled off zein film contains the intact gold layer. Even though there are some regions around the edges of the zein film pieces where gold layer is scratched off during cutting and peeling, the inverted nanostructure region (red square in Fig. 2c) is coated with gold perfectly without any defects as was shown before [17,27]. The fidelity of the transfer of the nanophotonic structures is further characterized with SEM imaging (Fig. 3). This gold coated zein surface was used for further decoration with gold, silver and silver-shelled-gold nanoparticles.

Fig. 3 shows the SEM images of the gold coated PDMS template with positive pyramid structures (a and b) and a zein based film with inverted pyramid structures that is peeled off from that PDMS template (c). The nanostructures are transferred with great fidelity and are all arranged in an orderly fashion consistent with our earlier work with this platform. Fig. 3b shows the surface deposition of gold with a nano granular structure which should facilitate the formation of hot spots. The inverted pyramid structures along with the gold layer were also successfully transferred on the zein film from PDMS as before [17].

The three different 20 nm nanoparticles (gold nanoparticles, silver nanoparticles and silver-shelled-gold nanoparticles) were diluted to the same concentration of  $7 \times 10^{10}$  particles/mL and were used for decoration of the surface of gold coated zein based inverted pyramid structures to study the relative enhancement of the Raman signal. The effectiveness of the binding of nanoparticles was also studied using SEM images. Fig. 4 shows the distribution of silver-shelled-gold nanoparticles on the surface of inverted pyramid structures. The SEM image

shows clustering of particles at different locations which brings them closer together in individual clusters rather than a uniform distribution of particles throughout the surface. The closeness of the particles facilitates the formation of hotspots and enhances the intensity of the Raman signal.

### 3.3. SERS measurement of Rhodamine 6 G on nanostructured, gold coated, nanoparticle decorated zein film sensor

First, Raman spectra of the nanoparticle decorated zein-based sensors were measured without Rhodamine 6 G (R6 G) to show the base signals of the sensors (Fig. 5). Also, as a reference, Raman spectra of concentrated aqueous cysteamine solution dried on a glass slide is given in Supplementary Fig. 2. All the sensors show some of the characteristic peaks of cysteamine in the Raman spectra in low intensities located at  $732\text{ cm}^{-1}$  (CS stretching),  $940\text{ cm}^{-1}$  (CCN stretching),  $1030\text{ cm}^{-1}$  (CCN stretching),  $2853\text{ cm}^{-1}$  ( $\text{CH}_2$  stretching) and  $2908\text{ cm}^{-1}$  ( $\text{CH}_2$  stretching) due to the presence of cysteamine in the design of the sensors [29]. Since cysteamine gives a peak of negligible intensity compared to Rhodamine 6 G, it is of no consequence in the detection of R6 G in this study.

Raman spectra of 10 mM Rhodamine 6 G (R6 G) on 1) a glass surface, 2) zein sensor surface with inverted nanophotonic structures and without any gold layer coating, and 3) zein sensor surface with 200-nm-thick gold layer coated inverted nanopyramid structures were measured to observe and compare the effects of nanostructures and the gold layer coated nanostructures (Fig. 6). R6 G was used at a concentration of 10 mM since lower concentrations did not provide enough intensity on samples without any gold addition. All three samples showed the characteristic peaks of R6 G which are approximately located at  $1513\text{ cm}^{-1}$ ,  $1364\text{ cm}^{-1}$ ,  $1314\text{ cm}^{-1}$ ,  $1183\text{ cm}^{-1}$ ,  $776\text{ cm}^{-1}$ , and  $616\text{ cm}^{-1}$  but with different intensities when compared to each other. 10 mM R6 G gave the lowest intensity peaks on the flat glass surface due to the absence of gold deposition and therefore no hotspot formation (Fig. 6A). Zein film with inverted nanostructures but without gold layer showed slightly higher intensities than flat glass surface due to the roughened surface with the nanostructure (Fig. 6B). The 200-nm-thick gold layer coated zein sensor surface with inverted nanostructures gave the highest intensities among these three samples, due to hotspot formation caused by the gold coated pyramid structures (Fig. 6C).

To calculate the SERS enhancement factor (EF) obtained with gold coated zein sensor compared to the flat glass surface, Eq. (1) was used using the intensities of the  $1364\text{ cm}^{-1}$  peak as the basis for comparison.

$$EF = \frac{(I_{\text{SERS}} \times N_{\text{NORMAL}})}{(I_{\text{NORMAL}} \times N_{\text{SERS}})} \quad (1)$$

$I_{\text{SERS}}$  is the intensity of  $1364\text{ cm}^{-1}$  peak of SERS measurement with 200-nm-thick gold layer coated zein sensor, and  $N_{\text{SERS}}$  is the number of R6 G molecules on this area.  $I_{\text{Normal}}$  is the intensity of  $1364\text{ cm}^{-1}$  peak on the flat glass surface without any gold deposition, and  $N_{\text{Normal}}$  is the number of R6 G molecules on this area. For calculating  $N_{\text{Normal}}$  and  $N_{\text{SERS}}$ , the number of R6 G molecules per unit sensor area with and without nanoparticles was calculated and multiplied with the Raman laser area. The relative EF in was calculated to be  $1.2 \times 10^3$ .

SERS enhancement effects using 100 mM R6 G for gold, silver and silver shelled gold nanoparticles on the gold coated nanostructured zein films are shown in (Fig. 7). Zein sensor decorated with silver-shelled-gold nanoparticles had the highest Raman enhancement, followed by the sensor decorated with silver nanoparticles. Zein sensor decorated with gold nanoparticles had the lowest enhancement effect among the three types of nanoparticles used.

To compare the SERS enhancements obtained with nanoparticle decorations only, enhancement factors for each type of nanoparticle decorated gold coated zein sensors were calculated in contrast to gold coated zein sensors using Eqn. 1. The enhancement factor relative to the gold coated nanostructured zein surface was  $3.29 \times 10^2$  for silver-

shelled-gold nanoparticles,  $2.88 \times 10^2$  for silver nanoparticles and  $2.46 \times 10^2$  for gold nanoparticles.

Fig. 7 also shows the different nanoparticle enhancement factors compared with zein film with nanophotonic structures only and without gold coating. The enhancement factor for silver-shelled-gold nanoparticles was  $1.26 \times 10^4$ . It was  $1.10 \times 10^4$  for silver nanoparticles and  $0.95 \times 10^4$  for gold nanoparticles. The enhancement factor substantially increased with the addition of the three sets of nanoparticles compared with zein with inverted pyramids coated with a layer of 200 nm of gold.

In order to compare the total zein film sensor ability as SERS substrate, we dropped three different nanoparticles directly on a glass slide and used it as the SERS substrate to detect R6 G (Fig. 8). The enhancement factor calculated between the silver-shelled-gold nanoparticle decorated zein sensor and silver-shelled-gold nanoparticle decorated glass slide was  $2.78 \times 10^3$  and was the highest among three types of nanoparticles. The enhancement was  $2.69 \times 10^3$  and  $2.12 \times 10^3$  for silver and gold nanoparticles respectively. The comparison of the enhancement factors shows the improvement of the Raman signal with the nanoparticle decorated nanophotonic structures on zein sensors.

In order to measure only the effect of nanophotonic structures, enhancement factors between the nanoparticle decorated 200 nm-gold layer-coated zein sensors were compared to those of nanoparticle decorated and 200 nm-gold layer coated flat glass slides (Fig. 8). The effect of nanophotonic structures were similar for all nanoparticle types. For the sensors decorated with silver and silver-shelled-gold nanoparticles the SERS signal was enhanced  $2.02 \times 10^3$  and  $1.99 \times 10^3$  times, respectively. For sensors decorated with gold nanoparticles, the nanophotonic structures enhanced the signal  $1.50 \times 10^3$  times. A comparison between Raman spectra of gold layer coated glass slides decorated with different nanoparticles are given in Supplemental Fig. 3. These enhancement factors show the importance of nanophotonic structures imprinted on zein film surface in creating hotspots to increase the sensitivity of the sensors.

The total enhancement factors of nanoparticle decorated zein sensor platforms were calculated using R6 G spectra on a flat glass slide without any gold nanoparticles. The highest enhancement factor of  $3.36 \times 10^5$  was obtained from silver-shelled-gold nanoparticle decorated zein sensor. Silver nanoparticle decorated zein sensor had a total enhancement factor of  $2.94 \times 10^5$ , and gold nanoparticle decorated zein sensor had a total enhancement of  $2.51 \times 10^5$ . All these total enhancements obtained with nanoparticle decorated zein sensor platforms are at least a decade higher than the previously obtained enhancement factor with gold coated nanostructured zein sensor [17].

The SERS enhancement factor obtained with the zein-based SERS biosensor platform in this paper is comparable to some of the other non-biodegradable SERS biosensor platforms. For example, the SERS enhancement factor of Au nanorod-covered  $\text{Fe}_3\text{O}_4$  microspheres used for the detection of a pesticide, thiram, was  $2 \times 10^5$ , which is very similar to the SERS enhancement of the zein-based SERS platform. In another study, Ag-Au bimetallic nanostructures were fabricated using a seeding technique and the highest SERS enhancement factor of  $10^4$  was obtained with gold ion to silver atom ratio of 4 [30], which is an order of magnitude lower than the zein based SERS platform enhancement factor in this paper. Bimetallic Ag-Au nanowires fabricated for the detection of a Raman active molecule, 4-MBA, in colloid solutions yielded SERS enhancement factors in the range of  $10^6$ - $10^7$ , slightly higher but still comparable to the SERS enhancement factor in this study [31]. There are of course, studies achieving higher SERS enhancement factors with the use of bimetallic nanoparticles with unique structures, such as a SERS enhancement factor of  $10^7$  was obtained with bimetallic concave gold and palladium nanostar structures [32]. Au or Ag deposited GaN nanoflowers gave enhancement factors of  $10^7$  [33]. In the detection of *p*-aminothiophenol, Ag-Au bimetallic hollow nanostructures reached an enhancement factor of  $10^8$  [34], and the use of bimetallic

Ag-Au nano-mushroom structures gave an enhancement factor of  $10^9$  [27]. Despite their higher SERS enhancement factors, fabrication of these SERS platforms usually necessitates the use of non-biodegradable metal, plastic or glass. The major advantage and uniqueness of the platform in this study is that it is largely (> 98 %) biodegradable. The biodegradable zein-based SERS platform fabricated in this paper offers a more sustainable alternative for non-biodegradable SERS platforms.

#### 4. Conclusion

This study aims to further increase the sensitivity of nanostructured zein-based SERS platforms by decorating the surface with gold, silver and bimetallic silver-shelled-gold nanoparticles to match the sensitivity of non-biodegradable, plastic-based SERS sensor platforms. The effects of silver, gold and silver-shelled-gold nanoparticles on the enhancement of the SERS intensity was investigated separately. Silver-shelled-gold nanoparticle decoration on the gold layer coated nanostructured zein platform gave the highest enhancement factor of  $10^5$  among all the nanoparticle types and made the SERS biosensor platform 100 times higher more sensitive than the previously developed zein based SERS platform [17]. This sensitivity improvement takes the newly developed zein based biodegradable SERS biosensor platform one step closer to non-biodegradable sensors and creates a new greener alternative.

#### Declaration of Competing Interest

None.

#### Acknowledgement

China Scholarship Council (CSC) provided a fellowship to Dr. Xiaoyuan Ma and a fellowship to Dr. Fei Jia to come to Purdue for a period of 12 and 18 months, respectively. The Purdue Scholle Endowment supported the research.

#### Appendix A. Supplementary data

Supplementary material related to this article can be found, in the online version, at doi:<https://doi.org/10.1016/j.vibspec.2019.103013>.

#### References

- [1] A.J. McQuillan, The discovery of surface-enhanced Raman scattering, *Notes Rec. R. Soc. Lond.* 63 (2009) 105–109.
- [2] T.-W. Chang, X. Wang, A. Mahigir, G. Veronis, G.L. Liu, M.R. Gartia, Marangoni convection assisted single molecule detection with nanojet surface enhanced Raman spectroscopy, *ACS Sens.* 2 (2017) 1133–1138, <https://doi.org/10.1021/acssensors.7b00427>.
- [3] H.-Y. Chen, M.-H. Lin, C.-Y. Wang, Y.-M. Chang, S. Gwo, Large-scale hot spot engineering for quantitative SERS at the single-molecule scale, *J. Am. Chem. Soc.* 137 (2015) 13698–13705, <https://doi.org/10.1021/jacs.5b09111>.
- [4] T. Gong, N. Zhang, K.V. Kong, D. Goh, C. Ying, J.-L. Auguste, P.P. Shum, L. Wei, G. Humbert, K.-T. Yong, M. Olivo, Rapid SERS monitoring of lipid-peroxidation-derived protein modifications in cells using photonic crystal fiber sensor, *J. Biophotonics* 9 (2016) 32–37, <https://doi.org/10.1002/jbio.201500168>.
- [5] K. Kneipp, H. Kneipp, I. Itzkan, R.R. Dasari, M.S. Feld, M.S. Dresselhaus, Nonlinear raman probe of single molecules attached to colloidal silver and Gold clusters, in: V.M. Shalaev (Ed.), *Opt. Prop. Nanostructured Random Media*, Springer Berlin Heidelberg, Berlin, Heidelberg, 2002, pp. 227–249, [https://doi.org/10.1007/3-540-44948-5\\_11](https://doi.org/10.1007/3-540-44948-5_11).
- [6] J. Prinz, C. Heck, L. Ellerik, V. Merk, I. Bald, DNA origami based Au–Ag-core–shell nanoparticle dimers with single-molecule SERS sensitivity, *Nanoscale* 8 (2016) 5612–5620, <https://doi.org/10.1039/C5NR08674D>.
- [7] T. Li, S. Vongehr, S. Tang, Y. Dai, X. Huang, X. Meng, Scalable synthesis of Ag networks with optimized sub-monolayer Au-Pd nanoparticle covering for highly enhanced SERS detection and catalysis, *Sci. Rep.* 6 (2016) 37092, <https://doi.org/10.1038/srep37092>.
- [8] O. Olea-Mejía, M. Fernández-Mondragón, G. Rodríguez-de la Concha, M. Camacho-López, SERS-active Ag, Au and Ag–Au alloy nanoparticles obtained by laser ablation in liquids for sensing methylene blue, *Appl. Surf. Sci.* 348 (2015) 66–70, <https://doi.org/10.1016/j.apsusc.2015.01.075>.
- [9] C. Zhang, S.Z. Jiang, C. Yang, C.H. Li, Y.Y. Huo, X.Y. Liu, A.H. Liu, Q. Wei, S.S. Gao, X.G. Gao, B.Y. Man, Gold@silver bimetal nanoparticles/pyramidal silicon 3D substrate with high reproducibility for high-performance SERS, *Sci. Rep.* 6 (2016) 25243, <https://doi.org/10.1038/srep25243>.
- [10] D.-K. Lim, K.-S. Jeon, H.M. Kim, J.-M. Nam, Y.D. Suh, Nanogap-engineerable Raman-active nanodumbbells for single-molecule detection, *Nat. Mater.* 9 (2010) 60–67, <https://doi.org/10.1038/nmat2596>.
- [11] L. He, M. Lin, H. Li, N.-J. Kim, Surface-enhanced Raman spectroscopy coupled with dendritic silver nanosubstrate for detection of restricted antibiotics, *J. Raman Spectrosc.* 41 (2010) 739–744, <https://doi.org/10.1002/jrs.2505>.
- [12] T. Yang, J. Doherty, H. Guo, B. Zhao, J.M. Clark, B. Xing, R. Hou, L. He, Real-time monitoring of pesticide translocation in tomato plants by surface-enhanced Raman spectroscopy, *Anal. Chem.* 91 (2019) 2093–2099, <https://doi.org/10.1021/acs.analchem.8b04522>.
- [13] T. Yang, Z. Zhang, B. Zhao, R. Hou, A. Kinchla, J.M. Clark, L. He, Real-time and in situ monitoring of pesticide penetration in edible leaves by surface-enhanced Raman scattering mapping, *Anal. Chem.* 88 (2016) 5243–5250, <https://doi.org/10.1021/acs.analchem.6b00320>.
- [14] L. Qiu, W. Wang, A. Zhang, N. Zhang, T. Lemma, H. Ge, J.J. Toppari, V.P. Hytönen, J. Wang, Core-shell nanorod columnar array combined with gold nanoplate–Nanosphere assemblies enable powerful in situ SERS detection of bacteria, *ACS Appl. Mater. Interfaces* 8 (2016) 24394–24403, <https://doi.org/10.1021/acsami.6b06674>.
- [15] J.-M. Li, Y. Yang, D. Qin, Hollow nanocubes made of Ag–Au alloys for SERS detection with sensitivity of  $10^{-8}$  M for melamine, *J. Mater. Chem. C* 2 (2014) 9934–9940, <https://doi.org/10.1039/C4TC02004A>.
- [16] H.-Y. Wu, B.T. Cunningham, Point-of-care detection and real-time monitoring of intravenously delivered drugs via tubing with an integrated SERS sensor, *Nanoscale* 6 (2014) 5162–5171, <https://doi.org/10.1039/C4NR00027G>.
- [17] P.G. Gezer, A. Hsiao, J.L. Kokini, G.L. Liu, Simultaneous transfer of noble metals and three-dimensional micro- and nanopatterns onto zein for fabrication of nanophotonic platforms, *J. Mater. Sci.* 51 (2016) 3806–3816, <https://doi.org/10.1007/s10853-015-9699-0>.
- [18] F. Jia, E. Barber, H. Turasan, S. Seo, R. Dai, L. Liu, X. Li, A.K. Bhunia, J.L. Kokini, Detection of pyocyanin using a new biodegradable SERS biosensor fabricated using gold coated zein nanostructures further decorated with gold nanoparticles, *J. Agric. Food Chem.* (2019), <https://doi.org/10.1021/acs.jafc.8b07317>.
- [19] H. Turasan, M. Cakmak, J. Kokini, Fabrication of zein-based electrospun nanofiber decorated with gold nanoparticles as a SERS platform, *J. Mater. Sci.* 54 (2019) 8872–8891, <https://doi.org/10.1007/s10853-019-03504-w>.
- [20] P.G. Gezer, G.L. Liu, J.L. Kokini, Detection of acrylamide using a biodegradable zein-based sensor with surface enhanced Raman spectroscopy, *Food Control* 68 (2016) 7–13, <https://doi.org/10.1016/j.foodcont.2016.03.002>.
- [21] P.G. Gezer, G.L. Liu, J.L. Kokini, Development of a biodegradable sensor platform from gold coated zein nanophotonic films to detect peanut allergen, Ara h1, using surface enhanced raman spectroscopy, *Talanta* 150 (2016) 224–232, <https://doi.org/10.1016/j.talanta.2015.12.034>.
- [22] E.A. Barber, H. Turasan, P.G. Gezer, D. Devina, G.L. Liu, J. Kokini, Effect of plasticizing and crosslinking at room temperature on microstructure replication using soft lithography on zein films, *J. Food Eng.* 250 (2019) 55–64, <https://doi.org/10.1016/j.jfoodeng.2019.01.018>.
- [23] S. Seo, T.-W. Chang, G.L. Liu, 3D plasmon coupling assisted sers on nanoparticle-nanocup array hybrids, *Sci. Rep.* 8 (2018) 3002, <https://doi.org/10.1038/s41598-018-19256-7>.
- [24] J. Shen, J. Su, J. Yan, B. Zhao, D. Wang, S. Wang, K. Li, M. Liu, Y. He, S. Mathur, C. Fan, S. Song, Bimetallic nano-mushrooms with DNA-mediated interior nanogaps for high-efficiency SERS signal amplification, *Nano Res.* 8 (2015) 731–742, <https://doi.org/10.1007/s12274-014-0556-2>.
- [25] S. Pande, S.K. Ghosh, S. Praharaj, S. Panigrahi, † Basu, S. Jana, A. Pal, T. Tsukuda, T. Pal, Synthesis of Normal and Inverted Gold–Silver Core–Shell Architectures in  $\beta$ -Cyclodextrin and Their Applications in SERS, (2007), <https://doi.org/10.1021/jp0702393>.
- [26] L. Wu, Z. Wang, S. Zong, Z. Huang, P. Zhang, Y. Cui, A SERS-based immunoassay with highly increased sensitivity using gold/silver core-shell nanorods, *Biosens. Bioelectron.* 38 (2012) 94–99, <https://doi.org/10.1016/j.bios.2012.05.005>.
- [27] E.A. Barber, Optimization of Zein Based Surface Enhanced Raman Spectroscopy Biosensor for the Detection of Gliadin As a Marker for Celiac Disease, Purdue University, 2018, <https://docs.lib.purdue.edu/dissertations/AAI10844563>.
- [28] F. Jia, E. Barber, H. Turasan, S. Seo, R. Dai, L. Liu, X. Li, A.K. Bhunia, J.L. Kokini, Detection of pyocyanin using a new biodegradable SERS biosensor fabricated using gold coated zein nanostructures further decorated with gold nanoparticles, *J. Agric. Food Chem.* 67 (2019) 4603–4610, <https://doi.org/10.1021/acs.jafc.8b07317>.
- [29] A. Kudelski, W. Hill, Raman study on the structure of cysteamine monolayers on silver, *Langmuir* 15 (1999) 3162–3168, <https://doi.org/10.1021/la9811463>.
- [30] X. Zou, E. Ying, S. Dong, Preparation of novel silver–gold bimetallic nanostructures by seeding with silver nanoplates and application in surface-enhanced Raman scattering, *J. Colloid Interface Sci.* 306 (2007) 307–315, <https://doi.org/10.1016/j.jcis.2006.10.084>.
- [31] S.E. Hunyadi, C.J. Murphy, Bimetallic silver–gold nanowires: fabrication and use in surface-enhanced Raman scattering, *J. Mater. Chem.* 16 (2006) 3929–3935, <https://doi.org/10.1039/B607116C>.
- [32] L.-F. Zhang, S.-L. Zhong, A.-W. Xu, Highly branched concave Au/Pd bimetallic nanocrystals with superior electrocatalytic activity and highly efficient SERS enhancement, *Angew. Chem. Int. Ed.* 52 (2013) 645–649, <https://doi.org/10.1002/anie.201205279>.
- [33] M.-R. Zhang, Q.-M. Jiang, Z.-G. Wang, S.-H. Zhang, F. Hou, G.-B. Pan, Three-dimensional gallium nitride nanoflowers supports decorated by gold or silver nanoparticles to fabricate surface-enhanced Raman scattering substrates, *Sens. Actuators B Chem.* 253 (2017) 652–659, <https://doi.org/10.1016/j.snb.2017.07.002>.
- [34] Y. Wang, H. Chen, S. Dong, E. Wang, Surface-enhanced Raman scattering of silver-gold bimetallic nanostructures with hollow interiors, *J. Chem. Phys.* 125 (2006) 044710, <https://doi.org/10.1063/1.2216694>.